

QUARK MATTER IN CORE COLLAPSE SUPERNOVA
SIMULATIONS*TOBIAS FISCHER^a, THOMAS KLÄHN^a, IRINA SAGERT^{b,c}
MATTHIAS HEMPEL^d, DAVID BLASCHKE^{a,e}^aInstitute for Theoretical Physics, University of Wrocław
pl. M. Borna 9, 50-204 Wrocław, Poland^bCenter for Exploration of Energy and Matter, Indiana University
2401 N. Milo B. Sampson Lane Bloomington, IN 47408, USA^cDepartment of Physics, Indiana University

727 E. Third St., Swain Hall West, Bloomington, IN 47405, USA

^dDepartment of Physics, University of Basel, Klingelbergstr. 82, 4056 Basel, Switzerland^eBogoliubov Laboratory for Theoretical Physics, JINR Dubna, 141980 Dubna, Russia*(Received February 14, 2014)*

Any reliable equation of state (EOS) for astrophysical applications faces recently severe constraints, in particular associated with high-precision observations of massive neutron stars. The associated stiffness of the EOS limits the freedom to include additional degrees of freedom at high density, *e.g.*, hyperons and quarks. For supernova matter, featuring high temperatures and large isospin asymmetry, there are only few EOS constraints at high density. We use this freedom and construct a quark–hadron hybrid EOS based on the bag model for strange quark matter. Parameters are selected such that (a) cold compact stars are consistent with observations and (b) quark matter appears close to saturation density. The hadron–quark phase transition is constructed by applying the Gibbs condition. This novel EOS is implemented in core-collapse supernova simulations in spherical symmetry, where we observe only a mild softening of the EOS in the quark–hadron mixed phase. The central protoneutron star (PNS) remains stable at all considered times and pure quark matter is never reached. The resulting slow conversion of nuclear matter into strange quark matter due to compression leaves a mild feedback to the neutrino observables as a consequence of the structural reconfiguration of the PNS. Moreover, we give a brief outlook towards more sophisticated quark–matter descriptions, *i.e.* the Nambu–Jona-Lasinio model and the Dyson–Schwinger formalism.

DOI:10.5506/APhysPolBSupp.7.153

PACS numbers: 95.85.Ry, 95.30.Qd, 95.30.Cq, 26.60.–c

* Lecture presented by T. Fischer at the XXXI Max Born Symposium and HIC for FAIR Workshop “Three Days of Critical Behaviour in Hot and Dense QCD”, Wrocław, Poland, June 14–16, 2013.

1. Introduction

Massive stars collapse at the end of their life due to weak processes, mainly electron captures on heavy nuclei, that remove pressure and lepton number from the stellar core [1]. The subsequent core compression continues until normal nuclear matter density is reached. It is the nuclear pressure from the highly repulsive short-range nuclear interaction that opposes gravity. The collapse halts and the core bounces back, which results in the formation of a hydrodynamic shock front. The central object which forms at core bounce is the PNS, it is hot and lepton rich in which sense it differs from neutron stars, the final supernova explosion remnant. The bounce shock propagation across the neutrinospheres releases an outburst of ν_e from a large number of electron captures on protons, leading to a rapid deleptonization where the electron fraction decreases to $Y_e \leq 0.1$. The resulting energy luminosity of several 10^{53} erg s $^{-1}$ lasts only about 5–10 ms. In combination with the continuous disintegration of heavy nuclei that collapse onto the shock from the still gravitationally bound layers above the core, the expanding bounce shock quickly turns into a standing accretion front. The later post bounce evolution $t_{\text{pb}} \geq 100$ ms is determined by mass accretion.

One of the largest uncertainty in studies that explore such evolution is the EOS at high densities, finite (and even high) temperature, and large isospin asymmetry or equivalent Y_e in the absence of any other negatively charged particles besides electrons. The corresponding conditions that supernova EOS must cover are illustrated in Fig. 1 of Ref. [2]. Many studies compared several different modern, mainly nuclear, EOSs at the level of spherical symmetry for massive stars that collapse to a black hole [3–6] as well as in axial symmetry [7, 8]. None of these papers explored the possibility of a phase transition to quark matter, for which it requires hybrid models that combine both hadrons (mainly nucleons) and quarks together with a phase transition construction. For that purpose, the simple quark-bag EOS has often been used in combination with hadronic relativistic mean-field EOS, to study the appearance and the possible impact of quark matter in supernova simulations [9–11].

Current constraints for nuclear as well as quark matter models are manifold. For example, nuclear constraints relate to the recent developments of chiral effective-field theory at intermediate densities up to saturation density [12, 13], and various new experimental results [14]. Moreover, current observational constraints point to a maximum neutron star mass above $2 M_\odot$ [15, 16] and radii of low-mass neutron stars between 10.4–12.9 km [17]. Unfortunately, the typically associated softening of the high-density EOS due to the appearance of quark matter, in particular strange quark matter, in many cases violates at least one of the aforementioned constraints.

2. Hybrid EOS consistent with current constraints

In order to be flexible in view of possible applications in astrophysics, but consistent with the current constraints of large maximum neutron star masses of $2.01 \pm 0.04 M_\odot$, we apply the simple but widely used quark-bag model for strange quark matter to construct supernova EOS. It is based on the free Fermi-gas model and determined from the two parameters bag constant, B , and corrections of the strong coupling constant, α_S (for details, see Refs. [2, 18]). We assume massless u and d quarks and a strange quark mass of $m_s = 100$ MeV. We select the hadronic EOS from Ref. [19] (henceforth denoted as STOS) which is based on the relativistic mean field (RMF) approach and Thomas–Fermi approximation for nuclear clusters. We combine baryon and quark EOSs via the construction of a phase transition applying Gibbs condition, for which conservation laws are always fulfilled globally and the pressure in the mixed phase is a strictly monotonous function of density. In order to be consistent with massive neutron star observations, we select the two parameters $B^{1/4} = 139$ MeV and $\alpha_S = 0.7$ (henceforth denoted as QB139 α_S 0.7). The resulting phase diagram and neutron star matter EOS ($T = 0$, β -equilibrium) are shown in Fig. 1. Under supernova conditions, *i.e.* temperatures of few tens of MeV and $Y_e \simeq 0.3$, the critical densities for the onset of quark matter is located around saturation density n_0 (solid/red line in the left panel of Fig. 1). Note that for symmetric matter ($Y_e = 0.5$) the critical density is in excess of $5 \times n_0$ (dotted/green

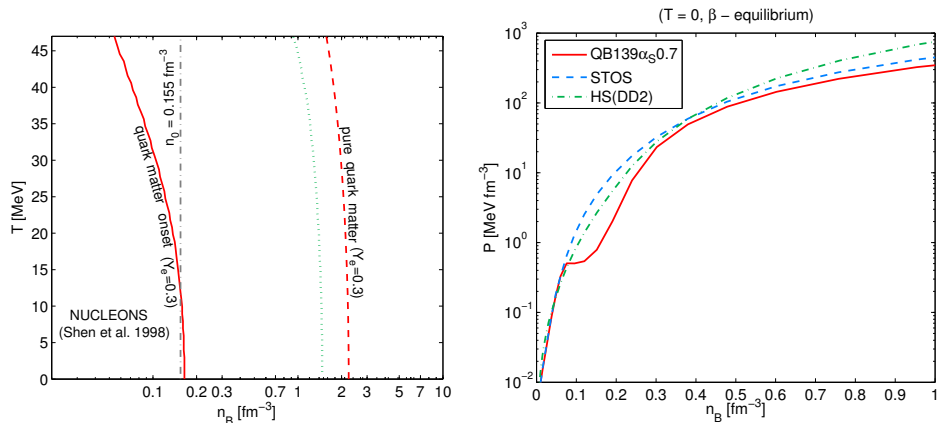


Fig. 1. Left panel: Phase diagram for the quark bag EOS (QB139 α_S 0.7) for $Y_e = 0.3$ (solid and dashed/red lines). For comparison, the onset conditions for symmetric matter ($Y_e = 0.5$) are also shown (dotted gray/green line). Right panel: EOSs for cold neutron stars in β -equilibrium, comparing QB139 α_S 0.7 (solid/red line), STOS [19] (dashed/blue line), and HS(DD2) [20, 22].

line in the left panel of Fig. 1). For these parameters, the very extended quark–hadron mixed phase stretches up to $10\text{--}14 \times n_0$ (depending on the temperature) above which pure quark matter exists (dashed/red line in the left panel of Fig. 1). For comparison, we also show the hadron EOS in the right panel of Fig. 1 (dash-dotted/green line), which is also based on the RMF approach with nuclear interaction DD2 [20]. We select it here because it was shown to be most consistent with current constraints [14], nuclear as well as observational (for a discussion, see Ref. [21]). The corresponding mass-radius curves are shown in Fig. 2.

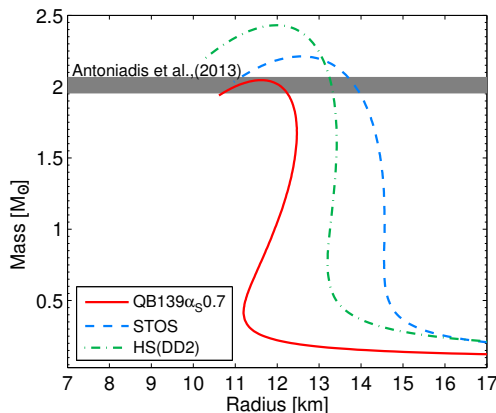


Fig. 2. Mass-radius relations for different EOS, comparing QB139 α_S 0.7 (solid/red line), the corresponding pure hadronic EOS STOS [19] (dashed/blue line), and for comparison also the EOS which is most in agreement with nuclear and observational constraints HS(DD2) (dash-dotted/green line). The gray vertical line marks the maximum compact star mass constraints of $2.01 \pm 0.04 M_\odot$ [16].

3. Hybrid EOS in supernova simulations

We implement this new quark bag EOS into our fully general relativistic core-collapse supernova code Agile-BOLTZTRAN which employs three-flavor Boltzmann neutrino transport (for details, see Ref. [23] and references therein). The list of the weak processes considered is given in Ref. [24]. Initial expectations based on Ref. [10], after which the PNS would collapse during the quark–hadron phase transition and produce an additional strong shock wave prior to the possible explosion onset, could not be confirmed with this hybrid EOS. The reason for the different evolutionary behavior of the PNS is related to the very broad mixed phase in which the EOS is softening only slowly, in comparison to previous studies where the also generally broad phase transition region was associated with a much more rapid softening [2, 10]. Here, the PNS core always stays in the mixed phase.

Nevertheless, the slow conversion of the hadronic PNS core into strange quark matter, on a timescale of hundreds of milliseconds after core bounce, leads slowly but constantly to a more compact configuration. It translates to higher central densities and temperatures, as well as lower Y_e , mainly due to the presence of strange quarks already at core bounce [21, 25]. We assume them to be produced from weak processes under the assumption of chemical equilibrium. The slow PNS compactification is accompanied by a changing neutrino emission characteristics. This is illustrated in Fig. 3 (black/red lines) in comparison to a simulation based on only hadronic EOS [19] (gray/blue lines). For the $11.2 M_\odot$ progenitor model under investigation [26], effects start to become visible at about 300 ms after core bounce and are noticeable for $t_{\text{pb}} \geq 600\text{--}800$ ms. The electron-flavor neutrino luminosities rise, by about 10–20% for ν_e and about 5% for $\bar{\nu}_e$, while the heavy lepton-flavor neutrino luminosity drops by about 5–10%. Hence, the originally very similar ν_e and $\bar{\nu}_e$ luminosities from the simulation with the purely hadronic EOS (gray/blue lines in Fig. 3) become clearly distinguishable. This enhancement of the accretion luminosities is related to the structural re-configuration of the PNS core and, therefore, well observable in the electron flavor neutrino fluxes. Moreover, the average neutrino energies generally rise, by about 2–3 MeV for ν_e and $\bar{\nu}_e$ and about 1–1.5 MeV for (μ/τ) –(anti)neutrinos.

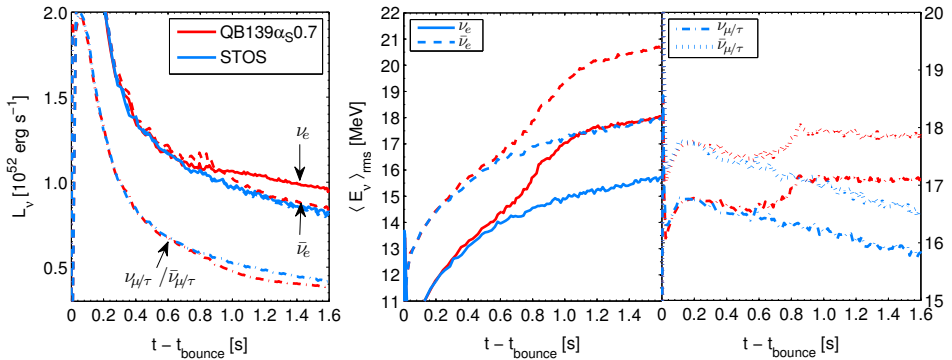


Fig. 3. Evolution of neutrino luminosities and average neutrino energies comparing a simulation with the purely hadronic EOS STOS (gray/blue lines) and quark–hadron hybrid EOS QB139 α_S 0.7 (black/red lines) which is based on the same hadronic model at conditions below the critical density for the onset of quark matter. All neutrino observables are identical during the early post bounce evolution during which quark matter is less abundant than 10^{-5} since the central density is not sufficiently high enough. With the phase transition, *i.e.* the onset of quark matter, after about 400 ms post bounce differences become noticeable and even large at later times.

4. Prospects on modeling quark matter in supernovae

Bag models have been developed to phenomenologically account for one of QCD's key features, namely the dissociation of hadrons into their constituent quarks at high enough pressure or temperature, *viz.* their deconfinement to quark matter. Introducing the bag constant is a simple approach to reflect the fact that hadrons during the transition to quark matter release confinement pressure, $B = P_{\text{conf}} - P_{\text{deconf}}$. While in vacuum, a corresponding value can be quantitatively determined from hadron properties (as done for the original MIT bag model) the in-medium deconfinement pressure can differ. More advanced approaches are likely to describe a bag 'constant', *viz.* the pressure difference between confined and deconfined phase, which actually depends on temperature, density and iso-spin asymmetry. The aforementioned α_S -corrections result from a perturbative treatment of QCD up to second order in the gluon coupling which result in differences to the actual free Fermi gas. While this approach is suited to sketch features of the deconfinement transition, it fails to describe the next important feature of QCD, the dynamical breaking or restoration of chiral symmetry which corresponds to the dynamic generation of quark mass due to the interaction via the gluon field. This effect is fully accessible only in a non-perturbative approach. The shortcoming of a perturbative correction treatment is reflected by the appearance of only constant quark masses in any bag model.

One approach to account for this non-perturbative feature is to apply the Nambu–Jona-Lasinio (NJL) model which starts from a phenomenological Lagrangian for quark matter and typically incorporates a contact interaction term between the quark fields which mimics the gluon mediated interaction. In this NJL framework, dynamical chiral symmetry breaking and hence the dynamical generation of quark masses is accessible. Depending on the chosen quark interaction channels and the corresponding coupling strengths, one can obtain EOS which are well suited to describe sufficiently large neutron star masses. This has been investigated in detail in two recent publications [27, 28] where the scalar, vector, and diquark coupling strengths have been systematically varied in order to identify parameter regions which support currently available phenomenological data, in particular the two recently reported massive neutron stars PSR J1614-2230 ($1.97 \pm 0.04 M_{\odot}$) [15] and PSR J0348-0432 ($2.01 \pm 0.04 M_{\odot}$) [16]. This demonstrates that there is no contradiction at all between these observations and the occurrence of quark matter described within the NJL model. It will be interesting to see how a hybrid EOS based on this approach in the quark sector will perform in supernova simulations similar to what has been described in the previous sections.

A potential shortcoming of this class of models should not be left unmentioned. The NJL Lagrangian can be motivated from QCD but is not directly related to the full Lagrangian of QCD. Hence, it almost certainly rather sketches what QCD might actually provide. For example, it is currently hard to grasp whether — and if so, how — confinement can be described within this framework. Moreover, hadrons are not explicitly included, *i.e.* quarks are the only degrees of freedom also at low densities. Another problem, typical for phenomenological approaches is the large amount of further possible interaction channels. Future studies will have to resolve which channels are relevant for observations. A small overview of possible additions to the interaction channels which have been investigated so far is given in reference [28].

A third possibility to address the properties of dense quark matter is based on the Dyson–Schwinger formalism which has been barely exploited for studies concerning quark matter at finite densities. It has been used widely and very successfully to explore vacuum and finite temperature properties of hadrons. The Dyson–Schwinger equations are non-perturbative equivalents of the Lagrange equations of motion in quantum field theory. Technically, one derives within the framework of the Green’s functions technique a set of coupled integral equations, the Dyson–Schwinger equations, from the QCD action. Both, confinement and dynamical chiral symmetry breaking are accessible. However, this approach is technically more demanding than the ones discussed so far and needs a careful analysis before it can be employed for detailed studies of supernovae. First steps towards an EOS within this framework can be found in [29, 30]. One of the notable results of these studies is the distinct non-free Fermi gas behavior of the one-particle quark distribution function in both references which might be important in dynamical scenarios as supernovae.

5. Summary

We have constructed a new quark–hadron hybrid supernova EOS, based on the quark-bag model for strange quark matter, consistent with observations of massive compact stars and radii of low/intermediate mass neutron stars. Note that if quark matter exists in nature, the most massive compact stars are the most likely candidates for hosting such exotic matter in their interior as they reach the highest core densities. As a novelty, we applied this hybrid EOS for core-collapse supernova simulations in spherical symmetry where neutrino-driven explosions cannot be obtained. We find that for our selection of quark matter parameters, the phase transition from nucleons to quarks starts around saturation density. In comparison to simulations that use the same hadronic EOS only, this leads to a faster compactification of

the PNS during the post-bounce evolution prior to the possible explosion onset. As a consequence of the applied Gibbs construction for the quark–hadron transition region in the phase diagram, we obtain an extended mixed phase (both, in terms of density and physical size). The EOS at the onset region of the mixed phase is very similar to the hadronic EOS, which in turn prevents the PNS core from developing a pure quark core. Instead, the PNS core stays at the onset of the mixed phase at all considered times. It never reaches higher densities within the mixed phase where the EOS is significantly softer. Therefore, no strong signal has been obtained, which is typically associated with the collapse of the PNS core during the phase transition. Nevertheless, it leaves a mild imprint in the neutrino emission. Even though it leaves the spectral differences unmodified, the increased magnitude of the average energies and the increased difference between the luminosities may be of relevance for neutrino oscillation studies and the nucleosynthesis. For the latter aspect, large (small) differences between the absorption rates for ν_e on neutrons and $\bar{\nu}_e$ on protons favors neutron (proton)-rich conditions [31].

We expect some of the features we describe to result solely from the existence of a phase transition region which is not necessarily related to the existence of quark matter. Further degrees of freedom, *e.g.* hyperons, are not unlikely to result in similar results. Further, we stress the point that this study is of a rather qualitative character and that further advances of our understanding of the EOS of dense and hot quark matter might lead to significant changes on both, a qualitative and quantitative, level. For this reason, we discussed alternative approaches to the in-medium description of quark matter, namely NJL-type models and the Dyson–Schwinger formalism.

T.F. and D.B. are supported by the Polish National Science Centre (NCN) within the “Maestro” program under contract No. DEC-2011/02/A/ST2/00306. D.B. and T.K. acknowledges also support from RFBR grant No. 11-02-01538-a. I.S. is thankful to the Alexander von Humboldt foundation and acknowledges the support of the High Performance Computer Center and the Institute for Cyber-Enabled Research at Michigan State University. M.H. acknowledges support from the Swiss National Science Foundation (SNF) under project number No. 200020-132816/1 and for participation in the ENSAR/THEXO project. The supernova simulations were performed at the computer cluster at the GSI Helmholtzzentrum für Schwerionenforschung GmbH, Darmstadt (Germany).

REFERENCES

- [1] H.-T. Janka *et al.*, *Phys. Rep.* **442**, 38 (2007).
- [2] T. Fischer *et al.*, *Astrophys. J. Suppl.* **194**, 39 (2010).
- [3] K. Sumiyoshi, S. Yamada, H. Suzuki, S. Chiba, *Phys. Rev. Lett.* **97**, 091101 (2006).
- [4] T. Fischer *et al.*, *Astron. Astrophys.* **499**, 1 (2009).
- [5] E. O'Connor, C.D. Ott, *Astrophys. J.* **730**, 70 (2011).
- [6] M. Hempel, T. Fischer, J. Schaffner-Bielich, M. Liebendörfer, *Astrophys. J.* **748**, 70 (2012).
- [7] A. Marek, H.-T. Janka, E. Müller, *Astron. Astrophys.* **496**, 475 (2009).
- [8] Y. Suwa *et al.*, *Astrophys. J.* **764**, 99 (2013).
- [9] K. Nakazato, K. Sumiyoshi, S. Yamada, *Phys. Rev.* **D77**, 103006 (2008).
- [10] I. Sagert *et al.*, *Phys. Rev. Lett.* **102**, 081101 (2009).
- [11] K. Nakazato, K. Sumiyoshi, S. Yamada, *Astron. Astrophys.* **558**, A50 (2013).
- [12] K. Hebeler, J.M. Lattimer, C.J. Pethick, A. Schwenk, *Phys. Rev. Lett.* **105**, 161102 (2010).
- [13] A.W. Steiner, S. Gandolfi, *Phys. Rev. Lett.* **108**, 081102 (2012).
- [14] J.M. Lattimer, Y. Lim, *Astrophys. J.* **771**, 51 (2013).
- [15] P.B. Demorest *et al.*, *Nature* **467**, 1081 (2010).
- [16] J. Antoniadis *et al.*, *Science* **340**, 448 (2013).
- [17] A.W. Steiner, J.M. Lattimer, E.F. Brown, *Astrophys. J.* **765**, L5 (2013).
- [18] S. Weissenborn *et al.*, *Astrophys. J.* **740**, L14 (2011).
- [19] H. Shen, H. Toki, K. Oyamatsu, K. Sumiyoshi, *Nucl. Phys.* **A637**, 435 (1998).
- [20] S. Typel *et al.*, *Phys. Rev.* **C81**, 015803 (2010).
- [21] T. Fischer *et al.*, *Eur. Phys. J.* **A50**, 46 (2013).
- [22] M. Hempel, J. Schaffner-Bielich, *Nucl. Phys.* **A837**, 210 (2010).
- [23] M. Liebendörfer *et al.*, *Astrophys. J. Suppl.* **150**, 263 (2004).
- [24] T. Fischer, G. Martínez-Pinedo, M. Hempel, M. Liebendörfer, *Phys. Rev.* **D85**, 083003 (2012).
- [25] A.W. Steiner, M. Hempel, T. Fischer, *Astrophys. J.* **774**, 17 (2013).
- [26] S. Woosley, A. Heger, T. Weaver, *Rev. Mod. Phys.* **74**, 1015 (2002).
- [27] T. Klähn, D. Blaschke, R. Lastowiecki, *Acta Phys. Pol. B Proc. Suppl.* **5**, 757 (2012).
- [28] T. Klähn, D. Blaschke, R. Lastowiecki, *Phys. Rev.* **D88**, 085001 (2013).
- [29] H. Chen *et al.*, *Phys. Rev.* **D78**, 116015 (2008).
- [30] T. Klähn *et al.*, *Phys. Rev.* **C82**, 035801 (2010).
- [31] Y. Qian, S. Woosley, *Astrophys. J.* **471**, 331 (1996).